Control Design for an Advanced Geared Turbofan Engine

Jeffryes W. Chapman[*]
Vantage Partners, LLC, Brook Park, OH, 44142, USA

Jonathan S. Litt[†]
NASA Glenn Research Center, Cleveland, OH, 44135, USA

This paper describes the design process for the control system of a next generation geared turbofan engine. This concept engine simulation is representative of a 30,000 lbf thrust class engine with two main spools, an ultra-high bypass ratio, and a variable area fan nozzle. Control system requirements constrain the non-linear engine model as it operates throughout its flight envelope of sea level to 40,000 ft and from 0 to 0.8 Mach number. The purpose of this paper is to review the engine control design process for an advanced turbofan engine configuration. The control architecture selected for this project was developed from literature and reflects a configuration that utilizes a proportional integral controller with sets of limiters that enable the engine to operate safely throughout its flight envelope. Simulation results show the overall system meets performance requirements without exceeding operational limits.

Nomenclature

AGTF30	Advanced Geared Turbofan 30,000
FMV	Fuel metering valve
HPC	High pressure compressor
HPT	High pressure turbine
LPC	Low pressure compressor
LPT	Low pressure turbine
MN	Mach number
OPR	Overall pressure ratio
PI	Proportional integral
PLA	Power lever angle
PR	Pressure ratio
SLS	Sea level static
SM	Stall margin
TIT	Turbine inlet temperature
Ts	Settling time
TSFC	Thrust specific fuel consumption
T-MATS	Toolbox for the Modeling and Analysis of Thermodynamic Systems
VAFN	Variable area fan nozzle
VBV	Variable bleed valve
N1	Low pressure shaft speed
N2	High pressure shaft speed
Nf	Fan shaft speed
Nfc	Corrected fan shaft speed
Ps3	Static pressure at engine station 3
T45	Temperature at engine station 45
W	Mass flow
Wc	Corrected mass flow

---

[*] Aerospace Engineer, 3000 Aerospace Parkway, Brook Park OH, AIAA Member.
[†] Research Engineer, 21000 Brookpark Rd., Cleveland OH, MS77-1, AIAA Senior Member.

American Institute of Aeronautics and Astronautics

Wf   Fuel flow

I. Introduction

As preparation for the next generation of high-efficiency aircraft engines continues, concept engine models are developed to offer researchers a simulation for development efforts. One such engine model is the Advanced Geared Turbofan 30,000 (AGTF30). The AGTF30 is a non-linear model of a 30,000 lbf thrust class engine that combines features such as a fan gearbox, variable bleed valve (VBV), variable area fan nozzle (VAFN), a relatively small engine core, and an ultra-high bypass ratio configuration, with a full control system. This paper describes the creation of the control system utilized in the AGTF30. The control system design approach is meant to enable stable and safe dynamic system operation, and follows a traditional engine control approach. Many descriptions of gas turbine control design can be found in literature.[1,2] This paper highlights the challenges that may be encountered with the features in this advanced engine design, and offers an example of a flexible engine test bed for advanced geared turbofan research.

The AGTF30 was implemented with MATLAB®/Simulink® and makes use of the Toolbox for the Modeling and Analysis of Thermodynamic Systems (T-MATS). T-MATS is an open source software‡ that facilitates the creation of thermodynamic systems that require external system solvers.[3] This modeling approach utilizes an energy balance method and component performance tables (maps) to define the non-linear turbo-machinery system. Engine architecture and performance capabilities for the AGTF30 are based on a concept engine developed by NASA Glenn Research Center and represent an advanced geared turbofan.[4,5,6,7] It should be noted that although development of the AGTF30 was based on the advanced geared turbofan in these references, it will not necessarily directly match them at any given operating point. Mismatch may occur because these are working models and are updated as new data become available. The AGTF30 simply offers a snapshot of the development of the advanced geared turbofan concept as of mid-2016.

The AGTF30 control system is representative of a traditional gas turbine engine control design. Engine effectors include fuel flow, a VBV, and a VAFN. Position of the VBV and VAFN effectors are determined by schedules developed from engine design criteria. The fuel flow control structure consists of a proportional integral (PI) feedback controller, and contains typical limiting logic to avoid engine dangers such as compressor stall/surge, over temperature, over speed, and combustor blow out.[8,9] Engine operating point is correlated with a corrected fan speed (Nfc) request signal that is compared to the Nfc derived from sensed signals from the engine. Fan speed request is set based on power lever angle (PLA) and is designed to linearly relate the position of a throttle to an output thrust.

Subsequent sections of this paper detail the development of the AGTF30 system. Specifically, discussion of the engine system architecture is located in Section II, followed by a description of the controller and how it was designed and integrated with the engine model in Section III. A mission performance analysis for the AGTF30 is presented in Section IV. Finally a summary of the paper is given in Section V.

II. Engine System Architecture

The AGTF30 is the simulation of a conceptual 30,000 lbf thrust class gas turbine engine containing high pressure, low pressure, and fan shafts (Figure 1). The low pressure shaft and fan shaft are connected by a gearbox with a 3.1 to 1 gear ratio, which acts to increase fuel efficiency and reduce gas turbine noise.[6] The low pressure shaft is powered by a low pressure turbine (LPT) and drives the fan and low pressure compressor (LPC). A VBV acts to reduce the possibility for LPC stall (i.e., improve stall margin (SM)) by diverting air from the exit of the LPC to the engine bypass stream, effectively lowering the LPC exit pressure.[1] The engine's small core includes a high pressure compressor (HPC), a combustion chamber, and a high pressure turbine (HPT) in series. Flow moving through the core exits through a conventional nozzle, while engine bypass air exits through a VAFN. The presence of a VAFN has many advantages that include, but are not limited to, improved engine efficiency and noise reduction.[5,10]

---

‡ https://github.com/nasa/T-MATS/releases , cited 10/2016

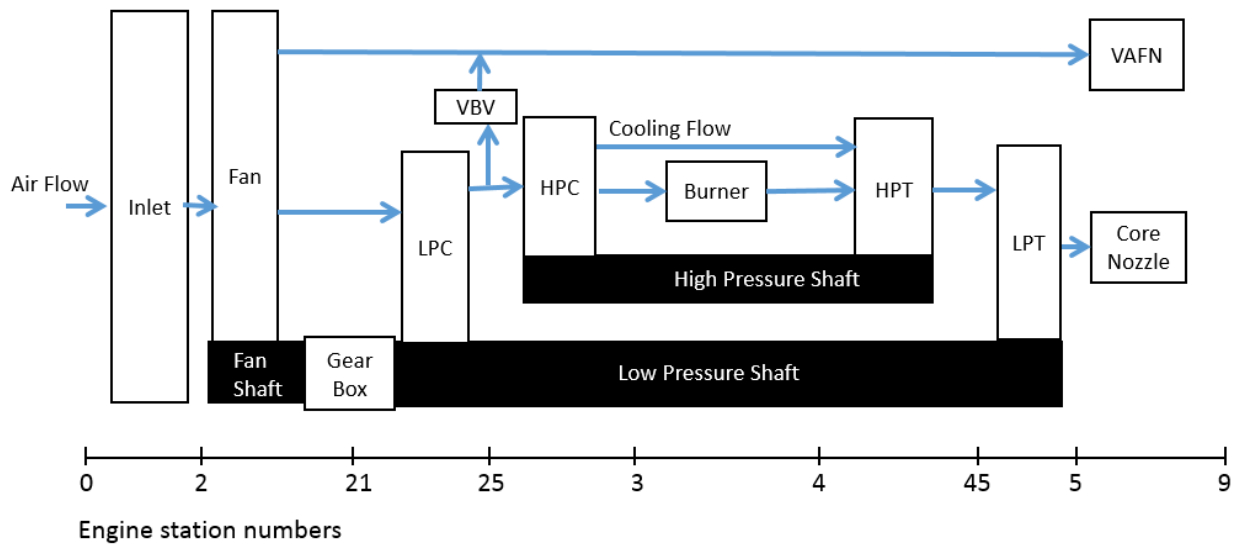American Institute of Aeronautics and Astronautics

Figure 1. Block diagram of the AGTF30 engine.

Performance characteristics of the AGTF30 can be seen in Table 1 for cruise and the hot day (27 degrees above standard day temperature) take off design conditions. From the table it can be observed that this is an ultra-high bypass ratio engine with a bypass ratio over 20, and demonstrates a thrust specific fuel consumption (TSFC) of less than 0.5 lbm/hr/lbf. These operating conditions are maintained by assuming engine design practices that enable increases in levels of overall pressure ratio (OPR) to over 50 and turbine inlet temperature (TIT) to over 3100 R for extended periods of time. Overall, this describes a highly efficient engine that would most likely be mounted on commercial vehicles and used on missions similar to those performed by the Pratt and Whitney PW1000G or CFM International LEAP products. It should also be noted that in this document, the high pressure shaft speed, low pressure shaft speed, and fan shaft speed will be known as N2, N1, and Nf, respectively.

Table 1. AGTF30 performance characteristics

Operating Condition	Air Flow, pps	TSFC, lbm/hr/lbf	Bypass Ratio	OPR	TIT, ºR	Thrust, lbf
Cruise at 35000 ft and 0.8 MN	813	0.4637	24	55	3150	6073
Max Thrust at hot day sea-level static (SLS)	1724	0.1751	28	37	3170	28622

III. Control System Architecture and Design

The control system for the AGTF30 engine was created around three main component types: the engine controller, the actuation system, and the sensors. The engine controller is modeled as sets of control algorithms. These algorithms determine the requested values for the engine control inputs: fuel flow, fan nozzle area, and LPC bleed valve position
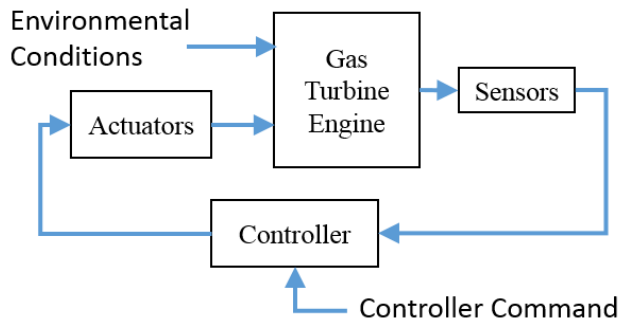
American Institute of Aeronautics and Astronautics

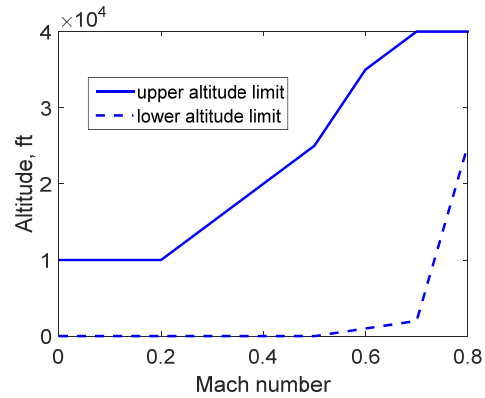**Figure 3. Diagram of overall AGTF30 engine system.**

Figure 2. AGTF30 operational envelope.

(expressed as a fraction of the full-open position). The sensors monitor the physical engine state and feed the values back to the controller. The actuation system represents the physical devices that act on the engine: fuel metering valve (FMV), VAFN, and VBV. A diagram of the overall model can be seen in
Figure **3**. The following subsections detail the design of each component. In these sections an operational envelope will be discussed. This envelope encompasses the environmental conditions in which the engine is expected to operate, as shown in Figure 2.

A. Fuel system control modeling

The engine fuel flow controller was constructed using the classical engine control architecture[2], as shown in Figure 4. With this controller structure, a PLA command is issued to the power management system, which translates the input to a requested value usable by the control system logic, in this case a fan speed request. A fan speed controller is then used to generate an ideal desired fuel flow or Wf request. Lastly, the final Wf demand is generated by comparing and adjusting the Wf request value to remain within the bounds of the fuel flow limiters, which act to maintain safe operation of the engine system.
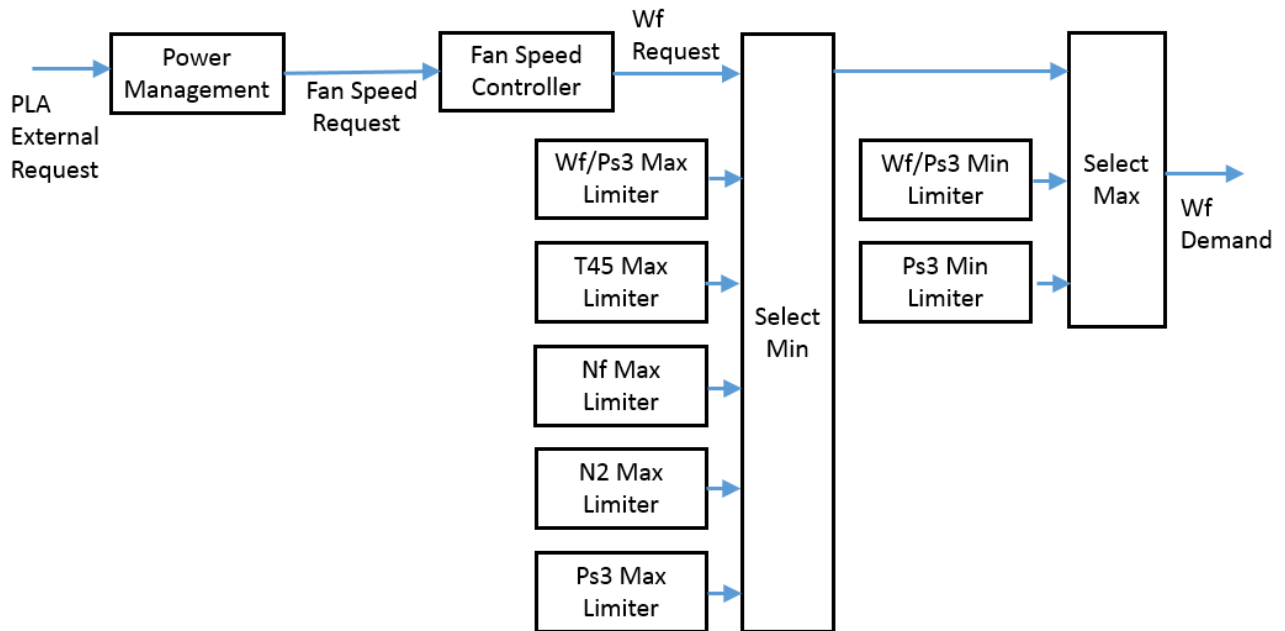

Figure 4. Diagram of AGTF30 fuel control logic.

4

For the AGTF30, linearity in the relationship between PLA and engine output thrust is a requirement. Unfortunately thrust cannot be directly measured, therefore the power management was designed to use Nfc as a thrust surrogate. There are several sets of sensors that can act as a stand-in for thrust in control systems. For the AGTF30, the engine speed sensor is selected because of precise and robust operation. Also, it correlates fairly linearly with thrust for a simple engine, as shown in Figure 5; this figure shows the relationship between Nfc and net thrust as occurs at the sea-level static (SLS) ambient condition (an altitude of 0 ft and Mach number (MN) of 0).

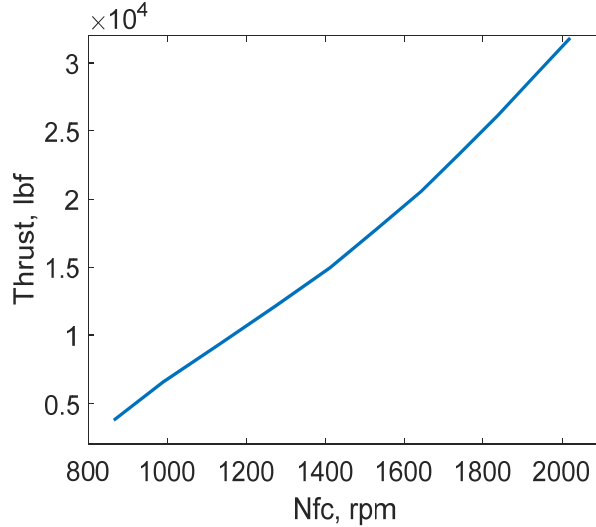To create the power management logic, the engine was used to generate Nfc values at many different thrust levels throughout the operational envelope. These values were then organized into a schedule that could be used to determine an Nfc value for any combination of altitude, MN, and PLA. So for any combination of inputs, the appropriate Nfc is found, and then adjusted using ambient temperature to obtain a final fan speed (Nf) request value to be issued to the fan speed controller.

Fan speed for the AGTF30 is maintained using a PI controller. Gains for this PI controller were developed using a two-step process. First, linear models of the engine were generated for points around the operational envelope. Second, gains for a PI controller were tuned, using the Edmund's method, for each generated linear model, to create a schedule of

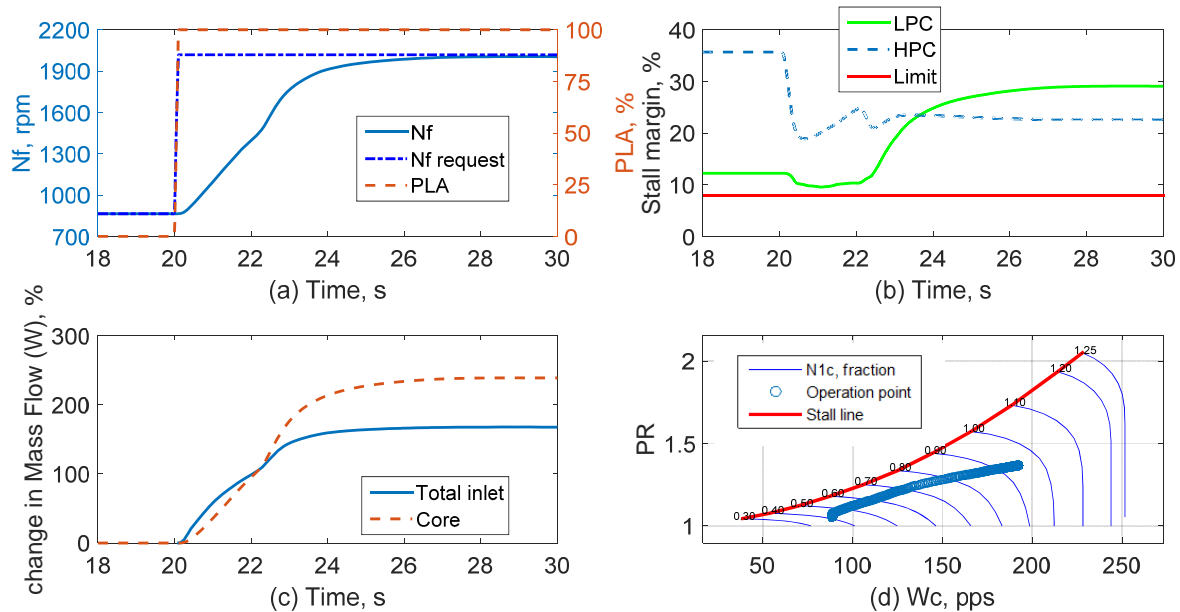**Figure 5. Relationship between Thrust and Nfc for the AGTF30.**

Figure 6. AGTF30 acceleration from idle to full power at SLS. Where (a) is the fan speed profile, (b) is the stall margin during the acceleration, (c) is the change in total and core only mass flow, and (d) is the LPC compressor operation line.

5

controller gains. The Edmund's method is a controller gain tuning technique that utilizes the least squares method to fit the proposed closed-loop system architecture to an ideal closed-loop system. [1, 11] In this case, the response of the linearized engine system with a PI controller was fit to an ideal second order transfer function by adjusting the controller gains. This second order transfer function was selected such that the gain and phase margins were greater than 6dB and 45°, respectively.[2]

Once the controller fan speed request is generated and PI fuel controller is tuned, the resulting fuel flow request is compared against a series of limits to determine the final fuel flow demand. Each limiter uses a PI controller and can be considered either steady-state or dynamic. Steady-state limits act to restrict engine operation during continuous operation. Dynamic limits act to restrict engine operation during transient operation. For this engine simulation, steady-state limits of maximum temperature at station 45 (T45) (as surrogate for temperature at station 4), Nf, N2, pressure at station 3 (Ps3), and minimum Ps3 were chosen. In this case the T45 limit was judged as the critical maximum limit and the Nf, N2, and Ps3 limits were inferred from T45 operational requirements. The minimum Ps3 limit was set at a level to maintain a reasonable idle thrust. Idle thrust level can change drastically with changes in engine architecture and is based on acceleration, temperature, and minimum stall margin requirements,[12] and was set at roughly 16% maximum thrust. In addition to the steady-state limiters, the controller contains two Wf/Ps3 limiters designed to keep engine acceleration within acceptable bounds. The max Wf/Ps3 ratio was set to limit acceleration with the goal of preventing stall while also allowing for acceleration from idle to 95% of takeoff power in 5 seconds. Values were determined by using the steady-state Wf/Ps3 values as a baseline, and increasing them until the acceleration requirement was met while also protecting arbitrary LPC and HPC stall margin limit of 8%. An acceleration from idle to full power at sea level and 0 MN can be seen in Figure 6. In this transient, a PLA command starts at idle (0%) and is raised to full power (100%) at 20 seconds (plot a). Stall margin in the LPC and HPC drop, but remain positive and above 8% (plot b). At 23 seconds the LPC stall margin can be seen to rise as the core air flow begins to increase more rapidly with respect to bypass airflow (plot c), and the LPC operation moves away from the stall line (plot d). The min Wf/Ps3 limit is typically set to limit deceleration with the goal of preventing loss of combustion in the burner. The AGTF30 model does not have the fidelity to predict loss of combustion events, therefore the min Wf/Ps3 limit was set mainly to improve robustness in model convergence during decelerations.

Transition between power management and limit logic is managed by an integral windup protection-based bumpless transfer logic. This logic was developed to seamlessly transition between the main fuel controller and the limit controllers. Because each controller contains an integrator (as part of the PI controller architecture), limiting integrator windup when a controller is not in use becomes paramount. A simple yet effective method for preventing integrator windup is to feed the final system demand (in this case Wf) back to the input of the controller, comparing this demand with the output of the controller, and then reducing the input to the integrator proportionally, as shown Figure **7**. For this application, the windup gain was selected using the relation found in literature,[13] shown in Eqn. (1).
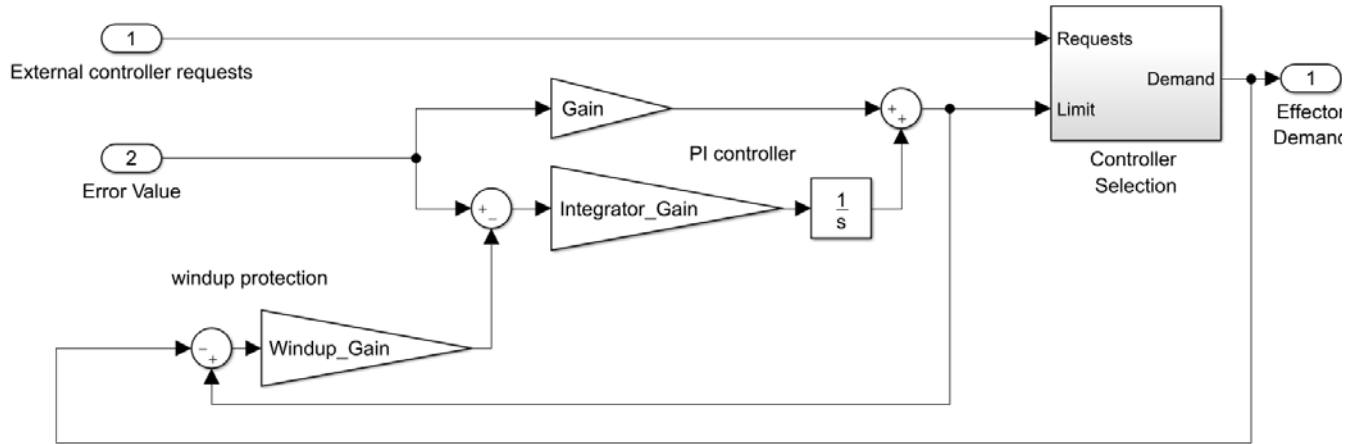

Figure 7. Notional diagram of bumpless transfer logic for AGTF30 controller transitioning.

$$SimulationTimeStep * Windup\_Gain * Integrator\_Gain < 1 \qquad (1)$$

B. Variable area fan nozzle control modeling

The VAFN is controlled to produce optimal fan performance at all operating points by maintaining a specific pressure ratio (PR) given a certain corrected flow (Wc) and Nfc. Optimal efficiency values were determined from the fan performance map (shown in Figure 8) and are represented as the fan operating line. It should be noted that map
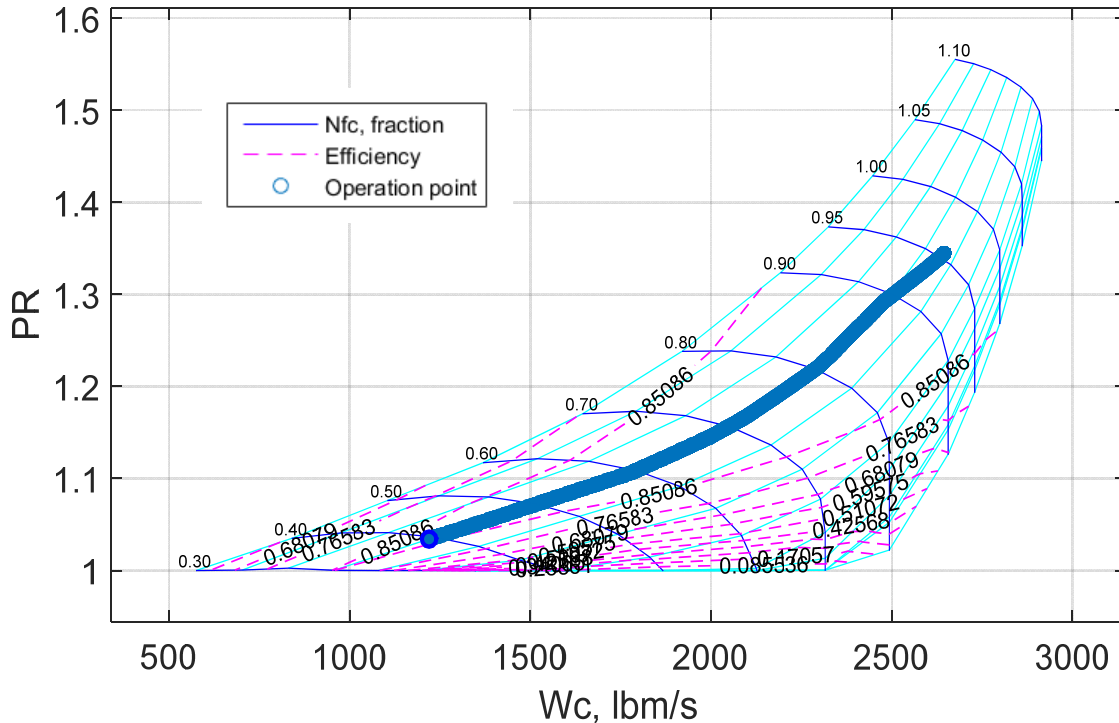

Figure 8. AGTF30 fan performance map with operating line.

values below Nfc of 0.5 (50% of the reference fan speed) have been extrapolated from the other values on the map. During operation, the VAFN area is adjusted to maintain the ideal fan operating line. Decreases in area leads to an increase in fan pressure ratio (PR), and vise-versa. To generate a schedule for the VAFN required area, the AGTF30 engine was run to steady-state at many different operating points, while VAFN was used to force the fan to the most efficient operating line. With these data, a table was created to relate VAFN position to MN and Nfc, as shown in Figure 9. In this figure it can be seen that at low MN the VAFN opens as Nfc is lowered, reducing the fan PR to avoid fan stall. In contrast, at high MN the VAFN is closed as Nfc is lowered, increasing PR to avoid fan choking. Current research into VAFN actuation has estimated that the maximum area reduction ratio (nozzle maximum scheduled area compared to the minimum scheduled area) achievable for nozzles is considered to be around 40%.[14] This maximum area was set taking into account only the most critical operating considerations. These are: potential fan stall during an idle to full power transient at MN = 0 and efficiency for cruise condition; and at high MN and high Nfc. Because the minimum area within these critical operating conditions is about 4500 in^2, the maximum area was set to 8000 in^2. Testing confirmed that stall margin with the limited area was acceptable for the associated speed and MN range. Larger area reductions beyond the 40% limit are also included to prevent the fan from choking. Fan choke is a less critical consideration, however operation under choke conditions can cause the simulation to become unstable so the conditions must be addressed in the model. These additional area reductions (areas below 4500 in^2) are beyond the capability of current designs and as such, prevention of fan choking will need to be examined further to explore the feasibility of a larger than 40% area reduction ratio or to research alternatives to avoid choking the fan, such as additional variable geometries or bleed flows. For the purposes of this futuristic concept engine model, this idealized VAFN throat area was deemed acceptable with the understanding that the model will be updated as more research becomes available.
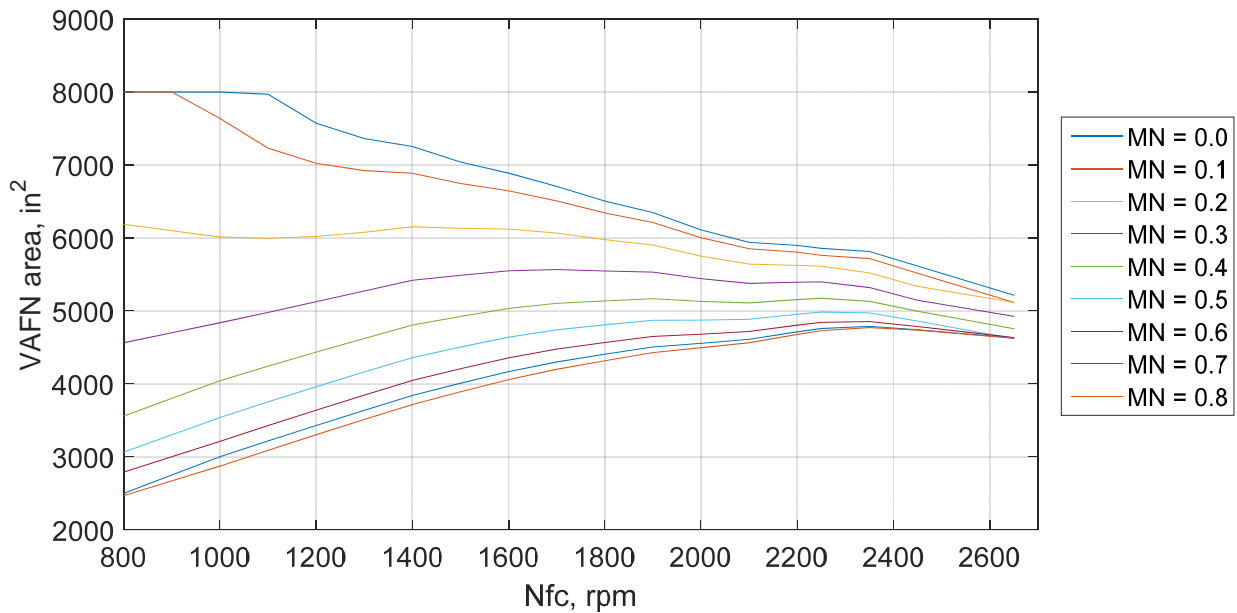
American Institute of Aeronautics and Astronautics

Figure 9. VAFN area vs Nfc and MN.

C. Variable bleed valve control modeling

The VBV is controlled to prevent LPC stall margin from going below 10% at steady-state. Similar to the VAFN, a schedule was developed to relate VBV position (fraction of full-open) to Nfc and MN within the operational envelope. The VBV schedule can be seen in Figure 10. At high Nfc values the LPC stall margin is close to 40%. As Nfc is decreased, the operating line moves closer to the stall line. At an Nfc of 1700 rpm, the VBV opens as stall margin approaches 10%. Once the VBV opens, it must continue opening at an increasing rate with respect to decreasing Nfc to maintain stall margin greater than 10%, as shown by the comparison of stall margin and VBV position in Figure 10.
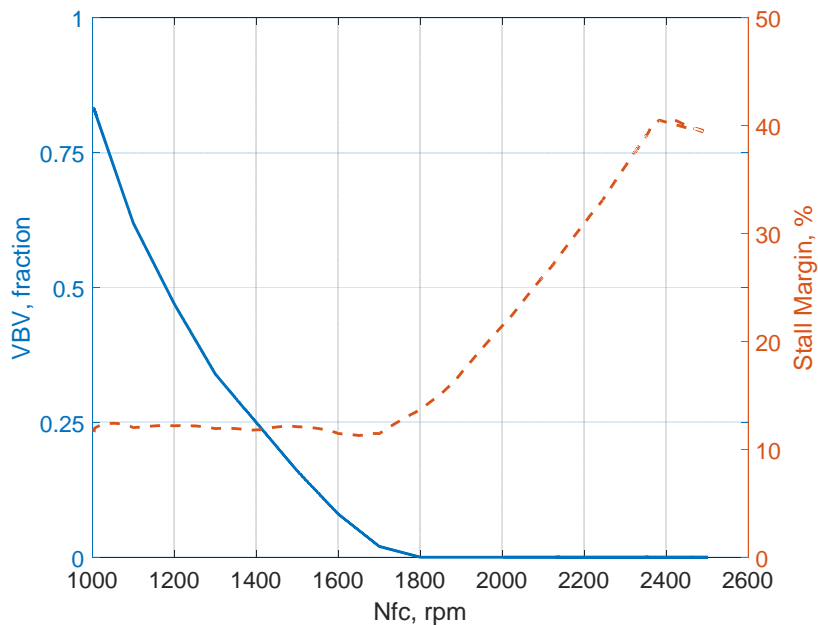

Figure 10. VBV and LPC stall margin vs. Nfc steady-state operational points at 35000 ft and 0.8 MN.

8

D. Actuator modeling

The actuator simulations have been constructed using simple first order models. The FMV and VBV actuators are represented with common dynamics defined by unity gain and a time constant as found in the literature.[1] The VAFN actuator is also modeled using a first order transfer function, however dynamics were defined based on a simple study. As with VAFN area, research in the actuation system is ongoing, and current VAFN research suggests potential use of shape memory alloys with response rates potentially too slow for required engine transients.[5] To determine the VAFN response time for the AGTF30 and a theoretical minimum requirement, the model was run with various VAFN settling times (Ts). These runs consisted of an acceleration from idle to full power at 10s followed by a deceleration from full power to idle at 70s, as shown in Figure 11. VAFN actuator settling times of 0.8s and 4s were chosen to allow close tracking of the controller demanded (ideal) area and to maintain a settling time comparable with the 5s acceleration requirement mentioned above, respectively. Values of 9.8s, 25s, and 45s were chosen based on plausible shape memory alloy slew rates.[5,12] In plot a the VAFN area for each run is shown, and it can be seen that the VAFN area is delayed as Ts is increased. Plots b and c show the effects of increasing VAFN delay as compared with ideal actuation. In plot b it may be observed that as VAFN delay is increased, fan speed during acceleration is increased; and conversely as fan speed is decreased, initially upon deceleration. This effect is caused by lower than designed pressure ratio during accelerations and higher than designed pressure ratio during decelerations, as the VAFN area is delayed in arriving at the designed area value. The additional effect of this delay is shown in the thrust (plot c), where there is loss of thrust during both accelerations and decelerations. This loss of thrust offers the main limitation of increasing the settling time of the VAFN, with Ts of 25s and 45s causing the engine to fail its requirement of 5s acceleration from idle to full power. Stall margin is also affected as shown in plot d, with lower stall margin during decelerations. Although this margin is lower, fan stall margin does not dip below 0, so it is deemed acceptable with all settling times tested. From this simple analysis, it was determined that the 9.8s Ts would be the minimum requirement for the VAFN actuation system with a baseline controller. If this performance cannot be met, advanced controls methods, such as model based engine control,[5] may be used to relax this requirement. Because the AGTF30 engine is a concept engine to be utilized for general research activities and due to the uncertainty of the actuator settling time, it was decided to proceed with an ideal settling time actuator. This faster response was deemed acceptable until more research on a feasible VAFN actuation system could become available.
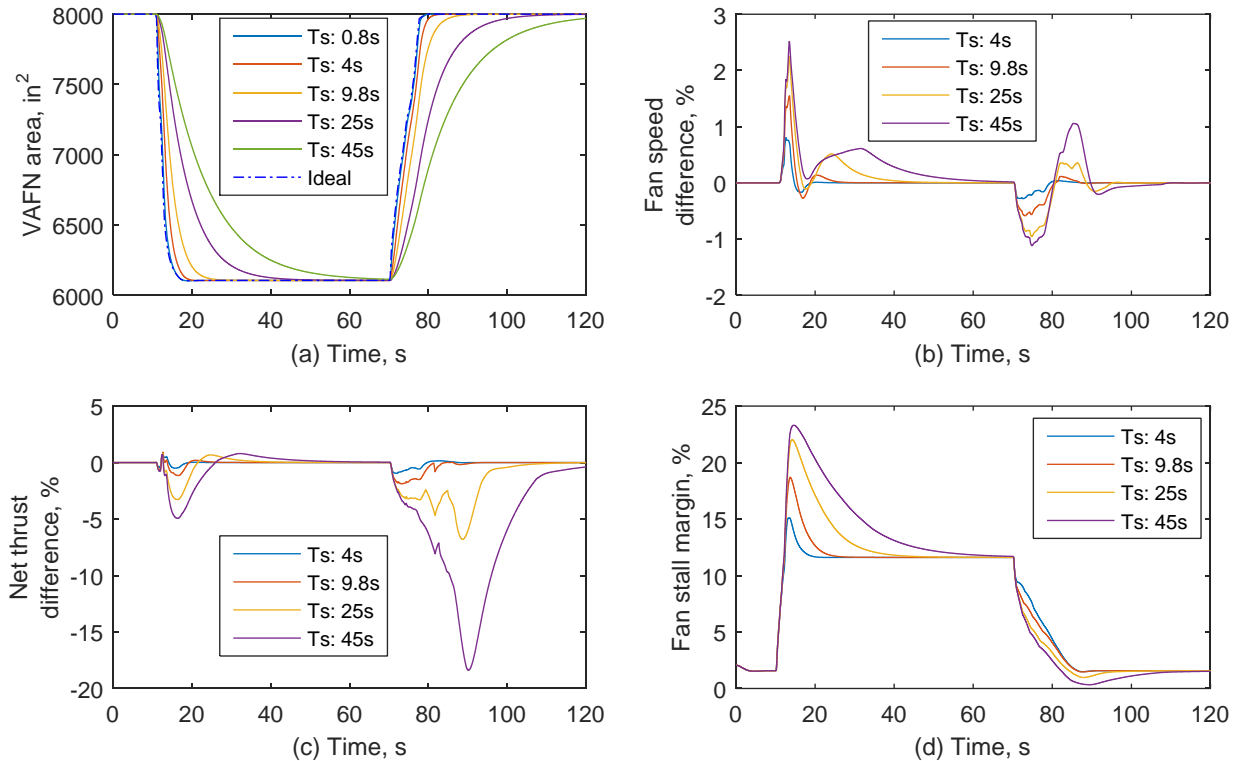

Figure 11. AGTF30 acceleration from idle to full power then deceleration from full power to idle.

9

American Institute of Aeronautics and Astronautics

E. Sensor modeling

All sensors are modeled with first order transfer functions defined by a gain and time constant. The gains for each sensor type were set to unity, and the time constants were determined based on general values found in literature.[1] As with the actuator models, the sensor models are meant to achieve a simple baseline of operation, and additional fidelity requirements will be assessed at a future date. The time constants for the sensors and actuators considered in this design are listed in Table 2.

Table 2. AGTF30 list of sensors and actuators. Note, fan shaft speed is derived from the low pressure shaft through the gear ratio

Sensors	Type	Location	Time Constant (s)
Pressure	Static	Ambient	1/25
Pressure	Total	Station 2	1/25
Pressure	Total	Station 25	1/25
Pressure	Static	Station 3	1/25
Pressure	Total	Station 5	1/25
Temperature	Total	Station 2	1/1.43
Temperature	Total	Station 25	1/1.43
Temperature	Total	Station 3	1/1.43
Temperature	Total	Station 45	1/1.43
Shaft speed		Low pressure shaft	1/50
Shaft speed		High pressure shaft	1/50
Actuators			**Time Constant (s)**
Fuel metering valve		Station 4	1/10
Variable bleed valve		Station 25	1/23
Variable area fan nozzle		Station 19	1/5

IV. Mission performance analysis

To demonstrate the capabilities of the AGTF30 engine simulation, a full flight mission profile was simulated. This flight profile was taken from a public source and contains mission data recorded onboard a regional commercial jet.[15] Traces of altitude, MN, and PLA are detailed in Figure 12 and show a typical 6000 s flight, including a take-off and landing. In the trace, take-off can be seen at about 800 s, followed by a climb to roughly 30,000 ft ending at 2000 s. At 4000 s a descent takes place with the aircraft landing at about 5250 s. Parameters of interest for the mission are shown in Figure 13. The variable geometry effectors (the VBV and VAFN) adjust from

Figure 12. Trace of common engine mission

idle to high power operation then back. Engine performance criterion TSFC is around 0.2 lbm/hr/lbf before take-off then moves to around 0.45 lbm/hr/lbf at cruise before returning to 0.2 lbm/hr/lbf as the engine drops altitude and lands. Parameter Ps3 increases sharply during take-off, reduces as altitude increases, and then fluctuates when the engine comes in for a landing as altitude drops and PLA is adjusted. Parameters T45, N1, and N2 largely follow PLA. Stall margins for the HPC and LPC show continuous operation below the operational stall line by at least 10%. The values demonstrate a typical engine mission transient and show the AGTF30's ability to operate safely and stably at all points.
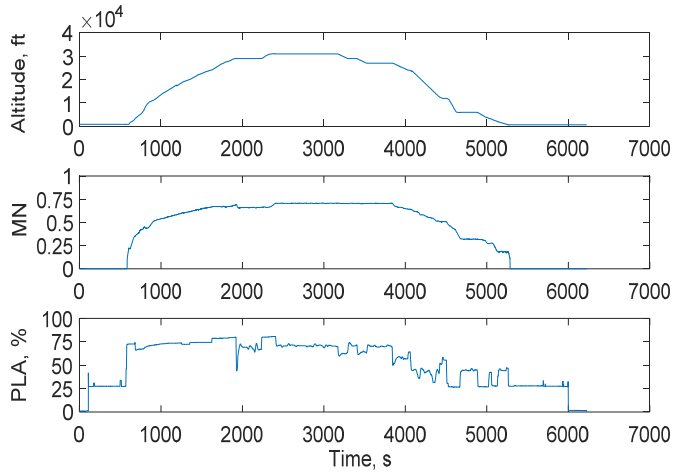
10

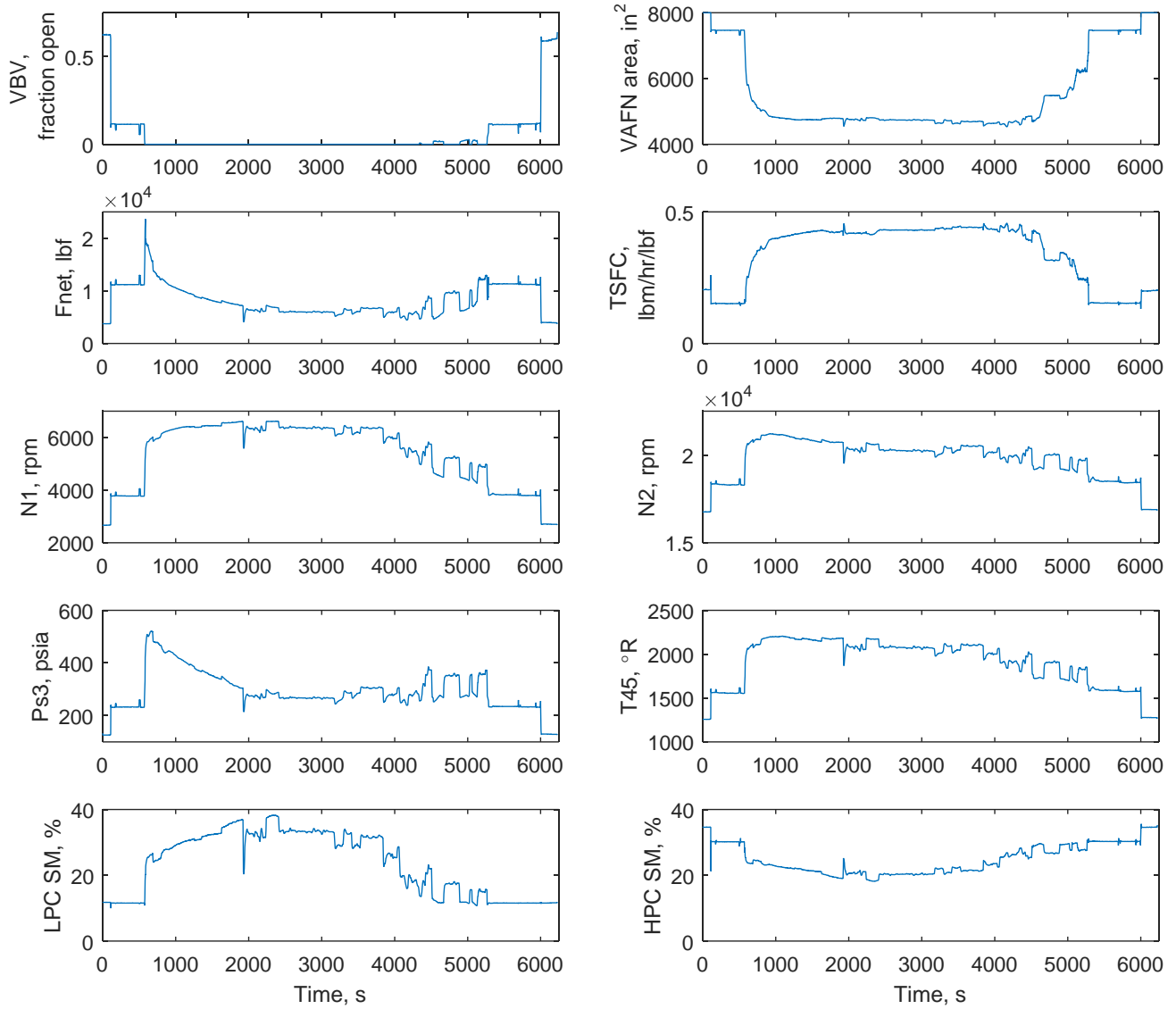American Institute of Aeronautics and Astronautics

Figure 13. Mission profile AGTF30 parameters.

V. Summary

This paper details the design of the controller for the Advanced Geared Turbofan 30k lbf (AGTF30) simulation, a conceptual geared turbofan engine created to represent an advanced/next generation aircraft engine. Special features of the AGTF30 include a variable area fan nozzle, variable bleed valve, gearbox connected fan, relatively small engine core, and ultra-high bypass ratio. The AGTF30 simulation was created in MATLAB/Simulink using the Toolbox for the Modeling and Analysis of Thermodynamic Systems (T-MATS) and is intended to provide a dynamic simulation of an advanced gas turbine that is operational throughout the full flight envelope. The control system for the AGTF30 follows a typical architecture with variable geometries controlled using scheduled values, and fuel flow controlled with the use of fan speed feedback, with sets of limiters that maintain safe operation. Full envelope control design was

American Institute of Aeronautics and Astronautics

accomplished by linearizing the engine model, then tuning sets of proportional integral controller gains, or by setting control schedules based on design criteria at each operational point. Review of the resulting parameters highlight the variable area fan nozzle design requirements for both nozzle area and nozzle slew speed may not be realizable at this time. A short study of the effects of different actuator slew rates with the baseline fan speed controller was conducted and minimum requirements for the actuator were detailed. Implementation of an idealized nozzle design was completed with the understanding that the model will be updated as future research into nozzle construction and/or advanced nozzle control is completed. Finally, a mission performance analysis was conducted on the AGTF30 engine system to demonstrate that dynamic system requirements are met. Simulation results show that the AGTF30 engine platform is a fully functional and dynamic engine platform that is capable of being used for advanced controls research on a next generation concept engine.

Acknowledgments

References

[1] DeCastro, J.A., Litt, J.S., and Frederick, D.K., "A Modular Aero-Propulsion System Simulation of a Large Commercial Aircraft Engine," AIAA -2008-4579, 44th AIAA/ASME/SAE/ASEE Joint Propulsion Conference & Exhibit, Hartford, CT, July 21-23, 2008.

[2] Csank, J., May, R.D., Litt, J.S., Guo, T.H., "Control Design for a Generic Commercial Aircraft Engine," NASA/TM-2010-216811, 2010.

[3] Chapman, J.W., Lavelle, T.M., May, R.D., Litt, J.S., Guo, T.H., "Toolbox for the Modeling and Analysis of Thermodynamic Systems (T-MATS) User's Guide," NASA/TM-2014-216638, 2014.

[4] Jones, S.M., Haller, W.J., Tong, M.T., "An N+3 Technology Level Reference Propulsion System", NASA/TM-2017-219501, 2017.

[5] Csank, J.T., Thomas, G.L., "Dynamic Analysis for a Geared Turbofan Engine with Variable Area Fan Nozzle," AIAA Joint Propulsion Conference & Exhibit, Atlanta, GA, July 10-12, 2017.

[6] Guynn, M.A., Berton, J.J., Tong, M.T., and Haller, W.J., "Advanced Single-Aisle Transport Propulsion Design Options Revisited," AIAA 2013-4330, AIAA Aviation, 2013 Aviation Technology, Integration, and Operations Conference, Los Angeles, CA, August 12-14, 2013.

[7] Hathaway, M.D., Del Rosario, R., and Madavan, N.K., "NASA Fixed Wing Project Propulsion Research and Technology Development Activities to Reduce Thrust Specific Energy Consumption," NASA TM 2013-216548, July 2013.

[8] Jaw, Link C., with Jack Mattingly, *Aircraft Engine Controls: Design, System Analysis, and Health Monitoring*, American Institute of Aeronautics and Astronautics, Inc, VA, 2009.

[9] Spang III, H.A., Brown, H., "Control of Jet Engines," Control Engineering Practice, Vol. 7, No.9, 1999, pp. 1043-1059.

[10] Michel, U., "The Benefits of Variable Area Fan Nozzles on Turbofan Engines," AIAA Aerospace Sciences Meeting including the New Horizons Forum and Aerospace Exposition, AIAA 2011-226, Orlando, FL, Jan 4-7, 2011.

[11] Maciejowski, J.M., *Multivariable Feedback Design*, Addison-Wesley, NY, 1989.

[12] Walsh, P.P., Fletcher, P., *Gas Turbine Performance*, 2nd ed., Blackwell Science and ASME, Fairfield, NJ, 2004.

[13] Martin, S., Wallace, I., Bates, D.G., "Development and Validation of a Civil Aircraft Engine Simulation Model for Advanced Controller Design," ASME Journal of Engineering for Gas Turbines and Power, Vol. 130, 051601-1-15, 2008.

[14] Song, G., Ma, N., Lee, H.-J., and Arnold, S., "Design and control of a proof-of-concept variable area exhaust nozzle using shape-memory alloy actuators," IOP Publishing, Smart Materials and Structures, Vol 16, pp 1342-1347, June 2007.

[15] Sample Flight Data." DASHlink -. Web. 04 April. 2017. https://c3.nasa.gov/dashlink/projects/85/resources/

American Institute of Aeronautics and Astronautics